# A FLUORESCENCE PHOTOBLEACHING STUDY OF THE MICROSECOND REORIENTATIONAL MOTIONS OF DNA

BETHE A. SCALETTAR, PAUL R. SELVIN, DANIEL AXELROD,* JOHN E. HEARST, AND MELVIN P. KLEIN

*Departments of Biophysics, Physics and Chemistry and Chemical Biodynamics Division, Lawrence Berkeley Laboratory, University of California, Berkeley, California 94720; and *Biophysics Research Division, Department of Physics, University of Michigan, Ann Arbor, Michigan 48109*

ABSTRACT We have conducted a polarized fluorescence photobleaching recovery (FPR) study of the rotational dynamics of ethidium azide labeled DNA. Polarized photobleaching experiments provide data on microsecond and millisecond molecular reorientation that complement the information available from nanosecond fluorescence depolarization studies. In polarized FPR experiments an anisotropic angular concentration of fluorophore is created by bleaching dye molecules in a preferred orientation with a short, intense pulse of polarized light. The sample is then weakly illuminated, and the temporal variation in the emitted fluorescence is monitored. The fluorescence signal will systematically change as molecules undergo post-bleach reorientation and the angular distribution of dye tends toward isotropy. We have observed that the time dependence of our microsecond FPR curves is also determined in part by nonrotational phenomena. To isolate the reorientational recovery we conduct our FPR experiments in two modes (called parallel and perpendicular) that differ only in the polarization of the bleaching light. A quotient function, $R(t)$, is constructed from the data obtained in these two modes; the variation with time of this new quantity is governed solely by processes that are sensitive to the polarization of the incident light (e.g., molecular rotation). It is found experimentally that $R(t)$ remains constant, as expected, for rotationally restricted DNA systems despite a temporal recovery in the parallel and perpendicular FPR curves. We also follow the dynamics of solutions of phage λ DNA as revealed in the temporal dependence of $R(t)$. This DNA system rotationally relaxes after ~100 μs and the dye/DNA complex reorients substantially during the 10-μs bleach period. Our FPR data are interpreted in terms of dynamic models of DNA motion.

## INTRODUCTION

An accurate description of DNA dynamics will considerably enhance our understanding of the molecular events that underlie the replication, transcription, and enzymatic recognition of nucleic acids. A considerable effort has, therefore, been directed at developing an accurate theoretical and experimental characterization of the intramolecular flexibility and Brownian diffusion of DNA. The following picture has been synthesized from the conclusions drawn in a number of studies of the motion of DNA in solution.

A substantial body of data supports the idea that DNA is a flexible polymer. The time-averaged dimensions of DNA have been characterized by measuring the radius of gyration, sedimentation coefficient, and intrinsic viscosity of the macromolecule (1). Very short pieces of DNA have been found to be rod-like in structure; however, as the molecular weight of the polymer increases the DNA begins to assume a bent conformation. The dynamics of DNA also reflect the flexibility of the molecule. Rigid rod diffusion models are capable of describing the rotational relaxation of only the shortest DNA fragments. Longer DNA molecules exhibit a complex spectrum of motions that includes nanosecond twisting of the helix axis, bending deformations, and slowly relaxing (millisecond) coil reorientations (2–17).

One of the most powerful tools used to monitor DNA motion is fluorescence spectroscopy. The picosecond fluorescence experiments of Magde et al. have provided evidence for rapid "wobble" in dye/DNA complexes (18). Fluorescence depolarization (FD) has been widely exploited in nanosecond studies of twisting deformations in nucleic acids (11–14). Austin and co-workers have demonstrated that a broad (nanosecond to millisecond) temporal range of DNA relaxations can be monitored by following the transient singlet depletion of a long-lived triplet probe (19). Unfortunately, in all of the above work, the use of a dye to monitor rotational motion has limited the experimentally accessible time regime to approximately the lifetime of the reporter molecule. Therefore, fluorescence spectroscopy has provided data primarily on those intramolecular motions of DNA that produce substantial angular displacement of the dye during its lifetime. In this work we report an application of fluorescence photobleaching spectroscopy (FPR) to the study of DNA rotation. The

photobleaching technique is not "lifetime limited" and is, in principle, capable of detecting any motion with a characteristic relaxation time that is longer than ~10 μs.

In polarized FPR experiments a short pulse of plane polarized laser light selectively destroys dye molecules whose absorption moments are oriented parallel to the polarization of the "bleaching" beam. A weak (probe) beam then monitors the return of an isotropic dye concentration as the bleached and fluorescent molecules reorient. FPR has been used to follow "slow" (≳100 ms) rotational relaxation in model membrane systems (20). The response time of our apparatus allows us to detect anisotropy decay that occurs over a time-scale longer than ~10 μs. In these experiments we were able to observe the reorientation of phage λ DNA for several hundred microseconds after bleaching the DNA sample. The FPR data also reflected the presence of more rapidly relaxing motions in our dye/DNA system.

## MATERIALS AND METHODS

### Ethidium Azide, DNA

The dye used in these experiments, ethidium monoazide, covalently binds to DNA upon photoactivation. Ethidium monoazide was synthesized and purified according to the procedure of Graves et al. (21). The product was characterized with mass spectrometry and visible absorption. Linear phage λ DNA was obtained from New England Biolabs (Beverly, MA). The azide was reacted with λ DNA (300 μg/ml in Tris-EDTA [TE] buffer, pH 7.5) by exposing dark incubated dye/DNA solutions to room light for 10 min. Unreacted azide was effectively removed by ethanol precipitation of the DNA.

The fluorescent properties of the covalently bound dye were monitored in a Fluorolog 212T (Spex Industries, Inc., Edison, NJ). Fluorescence excitation spectra of the photolysed dye/DNA complex indicated the presence of a single type of fluorescent species. The steady state polarization of the covalently bound dye was measured to determine the angle between the absorption and emission moments of the photoreacted fluorophore. In concentrated sucrose solutions the polarization was constant and very nearly 0.5 over the wavelength regime spanning the 514.5-nm electronic transition; therefore for this transition the absorption and emission dipoles are parallel.

In our experiments the ratio of dye to phosphate was ≲1/2,000. At such low loading ratios energy transfer between ethidium molecules is completely negligible. Photobleaching experiments were conducted on phage λ DNA solutions (2 mg/ml in TE buffer, pH 7.5, 50 mM NaCl).

We have also looked at samples in which the ratio of dye to phosphate was ≈1/1,000. However, as the dye level is raised the DNA becomes more difficult to resuspend after precipitation.

### FPR Experiments

Fast polarized FPR experiments were conducted in the laboratory of Daniel Axelrod. We present a brief discussion of the essential features of the apparatus (see Fig. 1). The excitation beam is the 514.5-nm line of an argon-ion laser (Coherent Inc., Palo Alto, CA). The light that emerges from the laser is deflected into a set of diffraction spots by an acousto-optic modulator. Only the first order spot is directed through an aperture; therefore, the intensity of the laser light incident on the sample is controlled by varying the amount of light sent into the first order deflection. During the bleach phase of an experiment the modulator directs ~50% of the light (2 W) into the first order; the probe beam is about 4,000 times less intense than the bleach.

Our photobleaching experiments are run in two alternate modes that

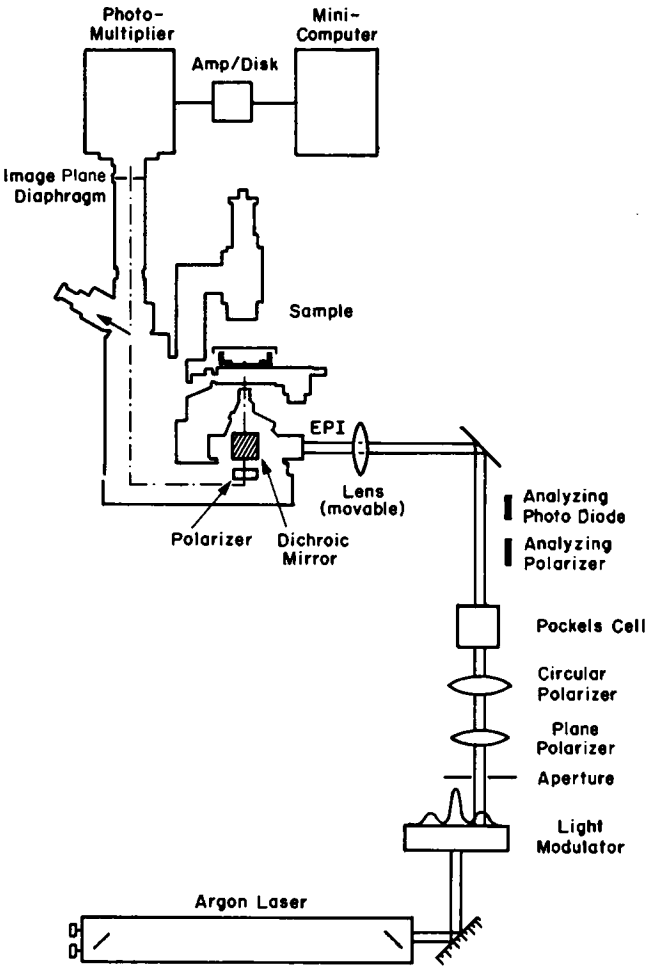


FIGURE 1 Apparatus used in fast rotational photobleaching experiments. The light source is a Coherent 15-W argon-ion laser. The beam emerges from the acousto-optic modulator as a series of diffraction spots. Note that the first order spot is directed through an aperture and onto the sample. During the probe phase of an experiment most of the light is contained in the zeroth order spot and therefore the sample is hit by a relatively weak beam. During the bleach pulse ~50% of the light is directed into the first order. To counteract depolarizing effects of the modulator the beam is sent through a plane polarizer; the light is then given a circular polarization by a quarter wave plate. At this point the beam is incident on a Pockels cell. The light emerges from the Pockels cell in one of two perpendicular plane polarized states. The output of the Pockels cell is monitored with the analyzing polarizer and photodiode. Several extra diaphragms are inserted along the beam path to block stray zeroth order light that passes through the first aperture. A movable lens is inserted before the microscope. The position of this lens will affect the size of the illuminated region of the sample. Finally, the light is directed onto the sample through a standard epi-illumination microscope set-up. In our experiments the ethidium azide labeled DNA was mounted on fused silica coverslips. In solution studies the sample was ~150-μm thick. The objective was always focused on the center of the sample to ensure that an image-plane diaphragm (see figure) blocked most photons emitted by any silica-bound DNA. A polarizer passes one polarization component of the fluorescence on to the phototube. The first stage of the photomultiplier is electronically gated to protect it from the bleach flash. The fluorescence photons are counted for intervals of 10-μs duration; the data are then stored in a NOVA 3/12 minicomputer.

differ in bleach beam polarization (see theory section for motivation). The direction of light polarization is controlled by a Pockels cell. The light that is sent into the Pockels cell has been circularly polarized by a quarter wave plate. The beam emerges plane polarized in one of two orthogonal directions. The probe beam always has the same polarization; the bleach is parallel to the observation (probe) beam in one mode and perpendicular to it in the alternate mode.

A series of secondary apertures are placed along the optical path. These extra diaphragms serve to block any residual zeroth order light that has passed through the first aperture. If zeroth order light is allowed to illuminate the sample, the contrast (the ratio of the intensities of the bleach and probe beams) is reduced. The contrast as well as the ratio of bleach intensity for the two possible bleach polarizations can be measured with an analyzing polarizer and photodiode.

The exciting laser light is directed onto the sample through an inverted epi-illumination microscope. The objective employed in these experiments had a magnification of 10 and a numerical aperture of 0.25. Typically the illuminated region was 3 $\mu$m in radius. The sample was mounted on fused silica to avoid background luminescence from glass which will persist for ~100 $\mu$s after bleaching.

In all the experiments described here, the sample was subjected to a 10-$\mu$s bleach pulse. The fluorescence intensity emitted by the sample under weak illumination was photon counted in intervals of 10-$\mu$s duration. The total experimental time after the bleach pulse was 1,500 $\mu$s (150 points at 10 $\mu$s/point); the pre-bleach fluorescence level was monitored for 200 $\mu$s (20 points at 10 $\mu$s/points). Only the $y$-polarized component (see next section) of the fluorescence is passed to the photomultiplier tube. There is a 10-$\mu$s delay between the end of the bleach and the onset of photon counting during the probe phase of the experiment. The bleach/probe cycle was repeated a minimum of 3,000 times on the same sample to assure the statistical significance of the curves; signal to noise was also improved with a 5 point cubic smooth of the data. The difference between the pre- and post-bleach fluorescence (normalized by the pre-bleach fluorescence) immediately after the 10-$\mu$s pulse will be referred to as the "depth of bleach." In our experiments the depth of bleach was typically between 0.35 and 0.60. The number of photon counts per second was ~150,000.

The microscope stage was minutely translated between each round of pulse/probe to avoid cumulative bleaching problems. Translation of the microscope stage serves to ensure that no point on the sample is exposed to bleaching light more than once. The quantum yield for the photodegradation of ethidium dye is known and it can be shown that a single exposure to our bleaching beam is insufficient to degrade the dye (22). Therefore, damage to the DNA which proceeds indirectly through the dye should not be a problem in these experiments. Moreover, there is no evidence for any light-induced breakage of the DNA in gels that we examine.

International Mathematical and Statistical Libraries (IMSL) routine ZXSSQ was used for all curve fitting. Data were fit to a single exponential of the form $A - B\exp(-t/\tau)$.

## THEORY

Polarized FPR has been applied to the measurement of "slow" rotational relaxation in a liposome system (20). In that work it was found that the characteristics of the FPR data were described by a theoretical model which attributes post-bleach anisotropy decay purely to molecular rotation. Here we will first review the theoretical ideas developed in reference 20. We then extend the theory of polarized FPR to deal with a more complex system in which there exist both rotational, and competing, nonreorientational processes in the sample. This generalized theory is the one that is applicable to the microsecond FPR study of DNA dynamics conducted here.

### Rotational Recovery in Millisecond FPR Experiments

Polarized photobleaching experiments typically are conducted in two modes (see Fig. 2). The fluorescent molecules are exposed to a very intense pulse of light that is polarized along the $y$ axis (parallel experiment) or the $x$ axis (perpendicular experiment). Immediately after bleaching, the intensity of the light is reduced by a factor of 4,000 and the temporal dependence of the fluorescence is then monitored. The polarization of the weaker (probing) beam is always parallel to the $y$ axis. Simple qualitative arguments suggest that the fluorescence intensity should rise as a function of time when an experiment is run in the parallel mode. In a parallel experiment the intense polarized light preferentially destroys dye molecules that are aligned along the $y$ axis at the time of the bleach. Moreover, during observation the probe beam will preferentially excite fluorophores that are oriented parallel to the $y$ axis. Immediately after the bleach the number of fluorescent molecules aligned parallel to the observation axis is

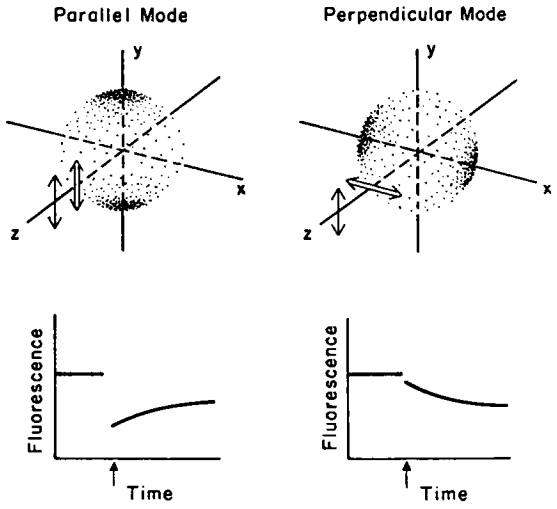


FIGURE 2 Schematic representation of the different bleach and probe events involved in the parallel and perpendicular modes of an FPR experiment. In the parallel mode an intense 10-$\mu$s pulse of light (⟷) creates a cylindrically symmetric pattern of bleached dye molecules about the $y$ axis. (We assume here that the system is static during the bleach.) The shading of the "darkness" profile indicates that fluorophores (absorption dipoles) that are parallel to the $y$ axis at the time of the bleach are most likely to be destroyed. In the parallel mode the observation beam (↔) preferentially excites dye molecules that are oriented along the direction of most intense bleaching. If post-bleach molecular rotation alone eliminates any anisotropy in the angular distribution of fluorophore the parallel mode FPR curve will exhibit a post-bleach recovery. In the perpendicular experiment the 10-$\mu$s pulse is polarized about the $x$ axis and therefore the bleach profile is also oriented about the $x$ direction. The observation beam preferentially excites dye molecules whose absorption dipoles are parallel to the $y$ axis. In the perpendicular mode the post-bleach signal decays as molecular rotation produces an isotropic distribution of dye. The rotational correlation times can be extracted either from the recovery of the parallel or the decay of the perpendicular curve.

reduced and therefore, initially, the fluorescence emitted by the sample under probe illumination is diminished relative to the pre-bleach level. As the bleached dye molecules begin to distribute themselves more uniformly over angular space, the parallel fluorescence rises (see Fig. 2). In a perpendicular experiment, one expects to observe a photobleaching decay curve since there is minimal destruction of fluorophores whose absorption dipoles are aligned along the observation axis (see Fig. 2); post-bleach molecular rotation serves, therefore, to reduce the number of fluorescent molecules that are parallel to the $x$ direction. These statements can be made mathematically precise for simple systems (20, 23, 24).[1] The analysis shows that the photobleaching curves will exhibit a bi-exponential recovery/decay in the parallel/perpendicular mode, respectively. As noted previously, these predictions have been qualitatively verified for a fluorescent liposome system where the relaxation times were several hundred milliseconds or longer (20).

## Rotational Recovery in Microsecond FPR Experiments

Our description of photobleaching curves has assumed that reorientational motion is the only physical process producing recovery. However, there may exist other mechanisms by which the fluorescence can recover (23).[1] Axelrod has noted that a bleached molecule (e.g., a dye/oxygen complex) might regain its fluorescent properties because the establishment of the nonfluorescent state is reversible.[1] Wegener and Rigler have suggested that if a complex multi-component system is under study the translational recovery of one species may overlap the rotational relaxation of a different component (23). The presence of competing recovery modes will clearly modify the predicted form of FPR curves. However, if we assume that only rotational processes are sensitive to the polarization of the incident light, there is a relatively straightforward way to isolate the component of the recovery that is derived from purely reorientational motion.

Wegener and Rigler (23) and R. E. Dale (24) have presented a method for separating the contributions of phenomena that do depend on orientation from those that do not. For the case where fluorescence is gathered by $4\pi$ steradian collection optics, only nonrotational processes contribute to the recovery if the observation beam polarization is rotated 54.7° with respect to the polarization of the bleach beam. The rotational motions are characterized from parallel and perpendicular FPR experiments and an anisotropy function is derived that is valid in the limit of shallow bleaches (23, 24).

For the very common case of epi-illumination microscope optics and arbitrary bleach depths, Axelrod has derived expressions for the ratio of parallel and perpendicular FPR data that likewise eliminates the orientation independent processes.[1] Since the experimental configuration that we use is the same as that analyzed in Axelrod's treatment a more detailed review of his results is presented.

Consider a quantity $R(t)$ defined as follows:

$$R(t) = \frac{F_0 - F_\perp(t)}{F_0 - F_\parallel(t)}. \tag{1}$$

Here $F_0$ denotes the pre-bleach fluorescence of the sample; $F_\perp(t)$ and $F_\parallel(t)$ refer to the post-bleach fluorescence at time $t$ in the perpendicular and parallel modes, respectively. The ratio $R(t)$ is predicted to start at a value less than unity at $t = 0$ (immediately after bleaching). This mathematical statement can be reformulated in a way that displays a clear analogy with the theory of pure rotational FPR. If $R(0) < 1$ we have $F_0 - F_\perp(0) < F_0 - F_\parallel(0)$, i.e., the depth of bleach is larger in the parallel mode than in the perpendicular. Hence, even if there exist nonrotational recovery modes for the sample we still expect the deepest bleach when the observation beam polarization (i.e., the direction of preferential excitation) is parallel to the direction of greatest bleaching. (Note in Fig. 2 that the bleach is also deeper for a parallel experiment when only rotational recovery is considered.) Then as time progresses and the bleached molecules distribute themselves uniformly over angular space $F_\parallel(t)$ and $F_\perp(t)$ will approach one another and the ratio will tend toward one. The time-scale associated with the rise of the ratio mirrors the purely reorientational processes in the sample.

Axelrod has made quantitative predictions for the behavior of the ratio $R(t)$ when the system is immobile on the time-scale of the fluorescence lifetime, and the bleach pulse, and when the molecules undergo isotropic spherical rotational diffusion in three dimensions (with diffusion constant $D_{rot}$) during the observation period. His results for the optical geometry used in these experiments are[1]

$$R(0) = 0.20 \tag{2}$$

and

$$R(t) = \frac{A - C\exp(-6D_{rot}t) - D\exp(-20D_{rot}t)}{A + 2C\exp(-6D_{rot}t) - \tfrac{8}{3}D\exp(-20D_{rot}t)}. \tag{3}$$

Here $A$, $C$, and $D$ are incomplete Gamma functions that depend on the depth of bleach. The ratio, however, is relatively insensitive to the depth of bleach (24).[1] It is also important to note that the magnitude of $D$ is generally much smaller than that of $C$. Expressions 2 and 3 are valid if the absorption and emission dipoles of the dye are parallel and the numerical aperture of the microscope objective is small. We note here that the term which decays as $-20D_{rot}t$ appears in the ratio because the FPR experi-

[1] Velez, M., and D. Axelrod, manuscript submitted for publication.

ment probes a more complex angular average than, for example, a fluorescence depolarization study. Hence neither the ratio, nor an FPR anisotropy function, evolves as a single exponential (see Appendix 1).

The reader may wonder why we have constructed a ratio, $R(t)$, from the parallel and perpendicular data rather than a traditional anisotropy, $r(t) = (\Delta F_\parallel - \Delta F_\perp)/(\Delta F_\parallel + 2\Delta F_\perp)$. Here $\Delta F_\parallel$ and $\Delta F_\perp$ are, respectively, the denominator and numerator of $R(t)$. In a fluorescence depolarization experiment the traditional anisotropy is "special" because its denominator is invariant as the fluorophores rotate. However, it is easily demonstrated that for our FPR geometry $\Delta F_\parallel + 2\Delta F_\perp$ is a function of $D_{rot}$. Therefore, the special position of $r(t)$ is not retained in our experiments and we have opted to use the simpler construct, $R(t)$.

In the next section and Appendix 1 the nature of the polarized FPR signal derived from a system of flexible macromolecules is considered. However, first we comment on simple generalizations of the microsecond FPR theory presented above. If the fluorophore undergoes azimuthally symmetric, restricted motion during the bleach, and if isotropic spherical rotational diffusion governs anisotropy decay during observation, the temporal dependence of the ratio is still that given in Eq. 3; however, the coefficients $A$, $C$, and $D$ are modified by the fast wobble. Of course, if the post-bleach relaxation mechanism is not strictly spherical rotational diffusion, a ratio expression of the form given above will not correctly described the system.

## Polarized FPR of Flexible Molecules

It has been noted that long DNA molecules exhibit a broad (nanosecond through millisecond) temporal spectrum of rotational motions. Therefore, Eq. 3 is certainly not expected to characterize these experiments. To formulate a realistic mathematical description of our signals one must invoke some model for the microsecond rotational dynamics of DNA. Unfortunately, the longer wavelength (microsecond) motions of higher molecular weight DNA are still somewhat incompletely understood. Therefore, a rigorous dynamic model of the FPR-DNA experiment is not presented. However, a formal analysis of the experiment, which illustrates the nature of the averaging problem at hand, is outlined in Appendix 1.

Qualitatively, we are able to say that the DNA will rotate during the bleach. Therefore, for these samples it is expected that the initial ($t = 0$) anisotropy in the angular distribution of dye will be less than that exhibited by a static system. However, if the DNA does not completely reorient on the time-scale of the FPR pulse, the sample should retain some anisotropy in the angular concentration of fluorophore at the end of the bleach. We can then follow the evolution of more slowly relaxing motions as the residual anisotropy decays.

It is now demonstrated that motion during the bleach pulse will raise the initial ratio above the static value of

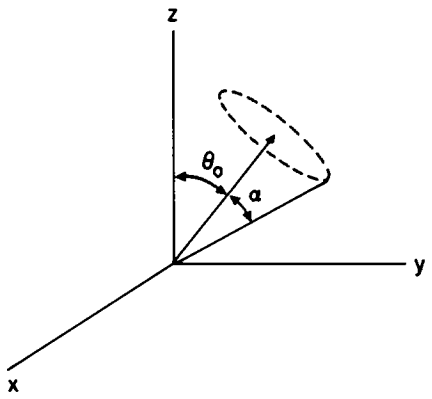


FIGURE 3 Mathematical basis for the wobble model of fast internal motion in a macromolecule. The absorption dipole is assumed to maintain an average angle $\theta_0$ with respect to the direction of polarization of the bleach beam (taken here as the $z$ axis for mathematical convenience). During the bleach period the absorption dipole uniformly explores a cone of half angle $\alpha$ centered about $\theta_0$. Therefore, the probability of absorbing the $z$ polarized light is not strictly proportional to $\cos^2\theta$ but must be computed as the average of $\cos^2\theta$ over the cone.

0.20. The proof is made by invoking a "uniform wobble in a cone" model (see Fig. 3 and Appendix 2). This "fast wobble" model will approximately describe motions that relax on a time-scale that is short relative to the fluorescence lifetime. A similar discussion has been presented for the photobleaching set-up using full $4\pi$ collection optics (23). Qualitatively, the existence of motion during the bleach will cause an increase in $R(0)$ because the distinction between the bleach profile in the parallel and perpendicular modes is reduced when a fluorophore wobbles and has increased probability of being destroyed by light of either polarization. If it is assumed that a dye molecule explores a cone of half angle $\alpha$ uniformly during the bleach then it can be shown that for our geometry

$$R(0) = \frac{1 - \chi^3/35}{2\chi^3/35 + 3\chi^2/5 + 1}. \quad (4)$$

Here $\chi = \cos\alpha(\cos\alpha + 1)$. Note that $R(0)$ is indeed an increasing function of $\alpha$ and that if $\alpha = 0$ we recapture the result $R(0) = 0.20$. Moreover, if the fluorophore moves very extensively during the bleach (i.e., $\alpha \approx 90°$), $R(0) = 1$ and the FPR technique is unable to resolve the rotational recovery of the molecule to which the fluorophore is attached.

## RESULTS

To test for the presence of nonrotational recovery processes in our DNA samples all FPR experiments were run, under identical conditions, in both the parallel and perpendicular modes. We found that the perpendicular curves did not exhibit a post-bleach decay (see Fig. 4). Therefore, the FPR data must be monitoring more than pure molecular reorientation and we focus attention on $R(t)$ to see what information about DNA rotation can be extracted from the temporal dependence of the ratio.

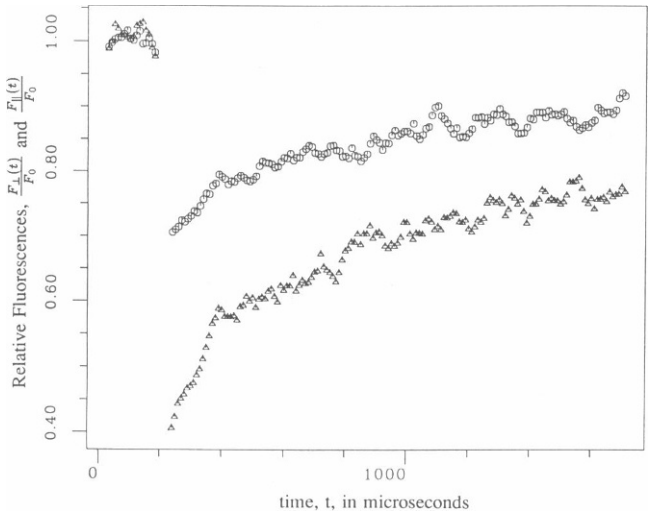


FIGURE 4 The parallel and perpendicular mode FPR curves for an immobilized DNA sample. The pre-bleach fluorescence level was monitored for 20 time points and is ~1 on the graph. Note that both parallel and perpendicular fluorescence signals recover but that the bleach depth is twice as large in the parallel experiment. Even in the presence of nonrotational recovery mechanisms if the sample retains some of the bleach pattern at an observation time $t$, the fluorescence signal at time $t$ must be lowest when excitation (i.e., the probe polarization) is along the direction of greatest bleaching. This physical argument is equivalent to our mathematical statement that $R(0) = (F_0 - F_\perp(0))/(F_0 - F_\parallel(0))$ is less than unity if the sample has not completely depolarized at the end of the bleach period. If $R(0) < 1$ then $F_0 - F_\perp(0) < F_0 - F_\parallel(0)$, i.e., the depth of bleach is larger in the parallel experiment than in the perpendicular.

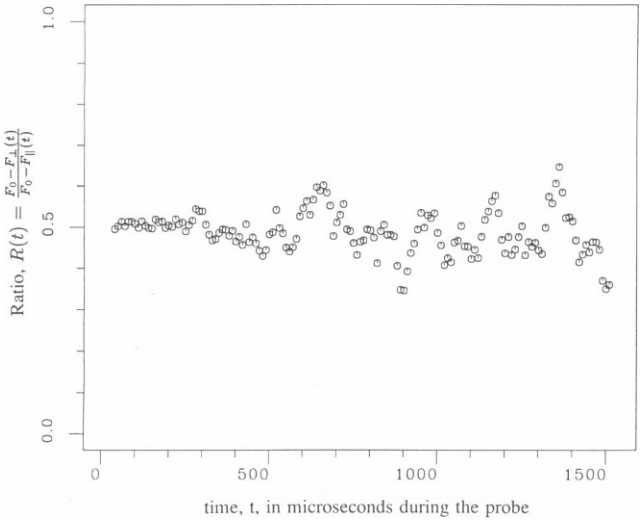


FIGURE 5 The ratio $R(t) = (F_0 - F_\perp(t))/(F_0 - F_\parallel(t))$ computed from the individual FPR curves shown in Fig. 4. As mentioned in the text $R(0)$ is ~0.5, and in fact the ratio does not differ significantly from 0.5 for the entire 1.5-ms observation period. Therefore, despite the fact the individual parallel and perpendicular FPR curves manifest some degree of recovery, the ratio exhibits the static behavior one would expect from a rotationally restricted sample.

Two classes of experiments were conducted in this study. First, we explored the polarized FPR data obtained from an immobilized DNA system. This simple experiment provides a test of the ability of the ratio method to monitor the bleach-induced anisotropy in the angular distribution of fluorophore. A value of $R(t)$ that is less than unity implies that the region of the sample under observation possesses (after the bleach) a nonuniform angular concentration of dye. Therefore, if at time $t$ the ratio is less than unity we conclude that the DNA molecule has not yet undergone complete post-bleach reorientation.

## Immobilized DNA Results

Phage λ DNA was dried onto fused silica coverslips and then subjected to a 10-μs bleach followed by a probe of 1,500-μs duration (150 points at 10 μs/point). An example of the individual parallel and perpendicular mode photobleaching curves obtained from such a sample is displayed in Fig. 4. It will be noticed that both the parallel and perpendicular curves exhibit a partial post-bleach recovery. The bleach is, however, twice as deep in the parallel mode. The ratio determined from such an experiment is shown in Fig. 5. Note that $R(0)$ is ~0.5 and that the "temporal evolution" of the ratio for the dry DNA sample is indicative of a highly immobilized system. The ratio is effectively constant over the entire 1.5-ms time interval under examination, hence we conclude that, in this sample, there are no large amplitude molecular reorientations that would allow the ratio to rise back up to unity.

## FPR on DNA Solutions

We have conducted a set of microsecond FPR experiments on DNA solutions. Examples of the data obtained when phage λ DNA (2 mg/ml in TE buffer) is subjected to a 10-μs bleach are displayed in Fig. 6. The observation time was ~1,500 μs. Note that both the parallel and perpendicular curves exhibit a partial recovery and that, once again, the bleach is deeper in the parallel mode.

The behavior of the ratio changes markedly when the DNA is suspended in solution. The initial value of the ratio increases to 0.87. Moreover, the ratio is not "static"; after ~300 μs $R(t)$ has risen back up to unity. To make this statement more precise a best-fit exponential has been drawn over the ratio. The exponential time constant, $\tau$, associated with the rise of the ratio was found to be 120 μs. We note that a single exponential function has been used to describe the evolution of the ratio because the scatter in the data is too great to warrant a more sophisticated, multiexponential fit. In fact, a complex superposition of relaxation processes undoubtedly governs the anisotropy decay. Both $R(0)$ and $\tau$ will be related to the dynamic behavior of the dye/DNA complex in the discussion section.

The success of these FPR experiments hinged on the use of a low power objective with a small numerical aperture. In our work with DNA solutions it was found that a high power objective (NA $\gtrsim$ 0.85) forces $R(0)$ toward unity; no dynamic information can then be extracted from the data.

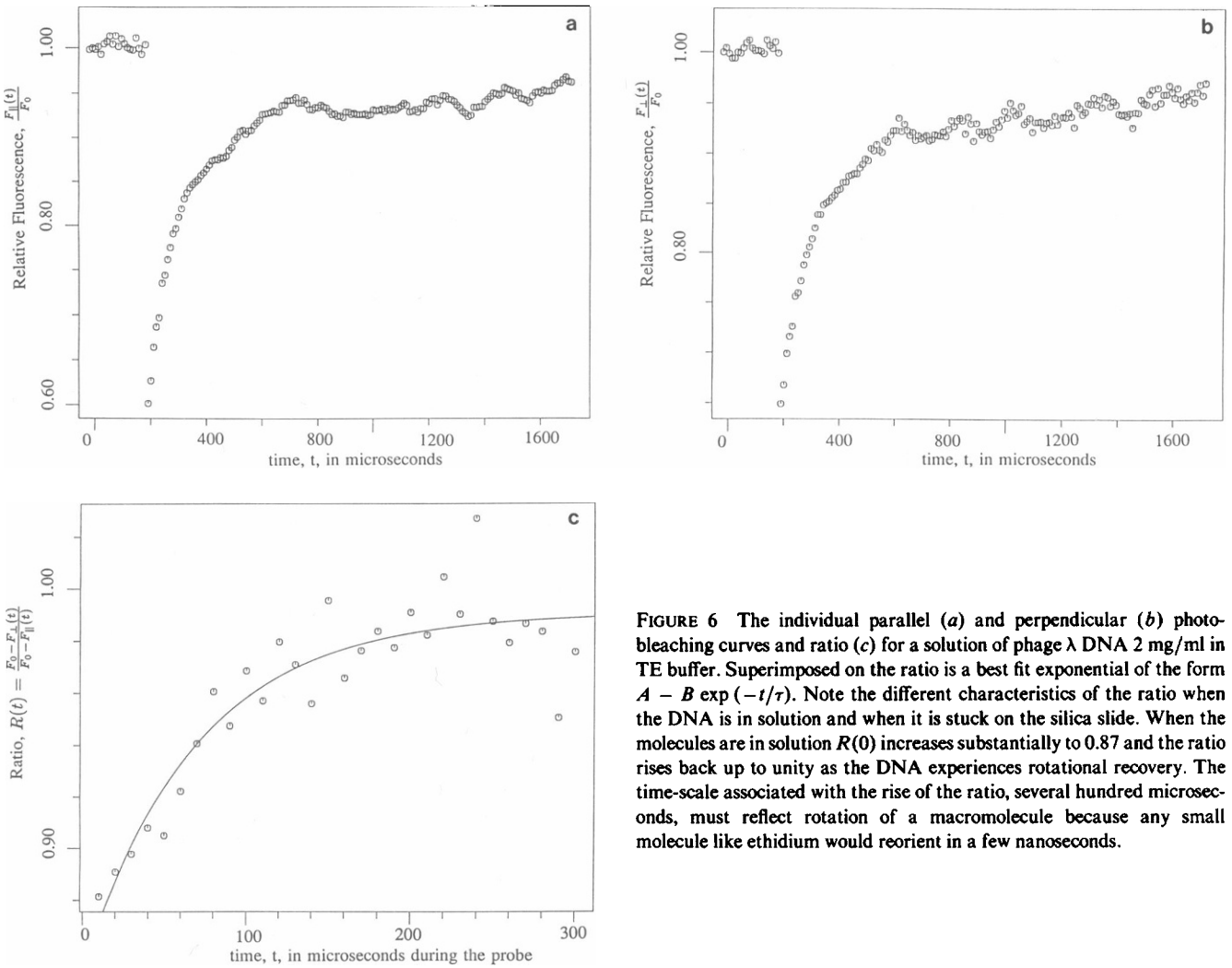


FIGURE 6 The individual parallel (*a*) and perpendicular (*b*) photobleaching curves and ratio (*c*) for a solution of phage λ DNA 2 mg/ml in TE buffer. Superimposed on the ratio is a best fit exponential of the form $A - B \exp(-t/\tau)$. Note the different characteristics of the ratio when the DNA is in solution and when it is stuck on the silica slide. When the molecules are in solution $R(0)$ increases substantially to 0.87 and the ratio rises back up to unity as the DNA experiences rotational recovery. The time-scale associated with the rise of the ratio, several hundred microseconds, must reflect rotation of a macromolecule because any small molecule like ethidium would reorient in a few nanoseconds.

## DISCUSSION

### Factors Affecting the Initial Ratio

Our measured value of $R(0)$ for a dry DNA system, 0.5, deviates substantially from the value of 0.2 predicted by a simple model in which it is assumed that the dye is static during the bleach and has parallel absorption and emission dipoles; the numerical aperture of the microscope objective is also assumed small. The rather high measured value for the initial ratio could have its origin in a number of phenomena. We discuss several possibilities. Residual dye motion in these "immobilized" samples could force $R(0)$ up to 0.5. For example, Eq. 4 may be used to demonstrate that "fast wobble" in a cone of half angle 45° will account for the observed values of $R(0)$.

The numerical aperture of the microscope objective also influences the initial value of the ratio. In our work with the 10× objective, this lens effect should raise the ratio <10% over the zero aperture value (20, 25).

For all immobilized samples the initial value of the ratio is found to be substantially <1. This fact argues strongly that an anisotropic angular distribution of dye is created by the bleaching light and is detected during the probe phase of the experiment. Moreover, if the system under study is expected to undergo complete rapid reorientation (on the nanosecond time scale) $R(0) = 1$ (i.e., no anisotropy remains at the end of the bleach[1]). Most probably some sort of residual motion of the dye or DNA is elevating the ratio above the theoretical lower bound.

### Statistical Significance of Results

It is important to demonstrate that the photon statistics in our experiments are good enough to make the conclusions reliable. We will present a detailed analysis of the data obtained from the DNA solutions. Once it is demonstrated that the ratio is statistically different from unity for the solution samples, it will be apparent that the ratio results are also significant in the case of the experiments on immobilized systems. Let us analyze the statistics of the first data point for the phage λ DNA solution. The total number of counts per second (pre-bleach) was ~150,000.

[1]Velez, M., and D. Axelrod, manuscript submitted for publication.

Hence in 10 $\mu$s the first bin accumulates about 1 photon. After an experiment is repeated 3,000 times there are 3,000 $\pm$ 55 counts at the first time point. Therefore the standard deviation in the counts divided by the pre-bleach is 0.012. Our data were given a 5 point cubic smooth; this improves the signal to noise by about a factor of $\sqrt{5}$. If the depth of bleach is 0.35 the relative uncertainty in the numerator, $(F_0 - F_\perp(0))/F_0$, of the ratio will then be $\sigma_{num}/\text{num} = 0.0054/0.35 = 0.016$. The depth of bleach is somewhat greater in the parallel mode (see theory section) but for our purposes here it is sufficient to say that the denominator is known to the same accuracy. The relative uncertainty in the ratio is then $\sigma_{rat}/\text{rat} = \sqrt{2}(0.016) = 0.022$. Finally, we conclude that $R(0) = 0.87 \pm 0.02$.

## Thermal Effects in Three-dimensional FPR Studies

In any FPR experiment it is necessary to analyze the magnitude of the light-induced thermal effects. Here we present a brief discussion of sample heating in three-dimensional FPR studies. In Appendix 3 we demonstrate that if the sample is infinite in extent the bleach-induced temperature rise, $\Delta T$, at the position of maximal light intensity is bounded above by the expression

$$\Delta T = \frac{9.2\epsilon CP}{\omega_0^2 \pi c_p \rho} \Delta t. \tag{5}$$

In Eq. 5 $\Delta t$ is the length of the bleach, $c_p$ is the specific heat of the sample, $\rho$ is the solution density, $\epsilon$ represents the extinction coefficient of the dye, $C$ is the concentration of the flurophore, and $\omega_0$ is the beam waist of the gaussian intensity profile of the laser light.

We will now use Eq. 5 to examine the importance of thermal effects in these experiments. The total laser power in the 514.5-nm line of the laser is 4 W. About 2 W is typically diffracted into the first order spot during a bleach. The beam waist was ~3 $\mu$m. The extinction coefficient of ethidium is $\sim 5 \times 10^3$ cm$^{-1}$M$^{-1}$. The dye concentration was ~1 $\mu$M and the sample thickness was ~150 $\mu$m. The thermal parameters of the solution are taken to be those of water. We find that $\Delta T = 0.8$°C. This calculation indicates that the samples were not heated excessively by the FPR bleach pulse.

## Effects of Numerical Aperture on the Ratio

During the early stages of the FPR work we tried to maximize the light intensity at the sample by focusing the laser with a high power objective. However, we had to abandon this approach because the use of a lens with a large numerical aperture tends to elevate the value of the ratio. The origin of this effect may be understood as follows. The theoretical analysis of polarized FPR assumes that all detected photons propagate parallel to the $z$ axis. Therefore, if the objective collects light traveling in directions that deviate substantially from the $z$ axis, the ratio will differ significantly from the theoretical zero numerical aperture limit. It can be shown that the ratio will increase as the numerical aperture of the lens goes up (20, 25). Therefore, for mobile systems that have intrinsically high ratios and ample fluorescence, it is advantageous to focus the laser light with a low power objective.

## Dynamic Interpretation of Decay/Relationship to Other Work

Here the FPR anisotropy decay is related to the twisting, bending, and coil (see below) deformation dynamics of $\lambda$ DNA. In particular, we indicate in what "experimental time-regime" each class of motion is expected to influence the FPR signal.

We first consider the possibility that the dye/DNA complex reorients considerably during the bleach period. The initial value of the ratio, 0.87, for a solution of phage $\lambda$ DNA is substantially larger than the "static" $R(0) = 0.2$; hence, the data suggest that the dye/DNA complex exhibits a substantial degree of motion during the bleach pulse.

Twisting motions of the dye/DNA complex are expected to contribute substantially to the unresolved component of the FPR anisotropy decay. We rationalize this statement as follows. The torsional reorientation of DNA has been the subject of extensive theoretical study (26–29). It is generally believed that DNA can be characterized by a torsional rigidity, $\alpha = 3.8 \times 10^{-12}$ dyn-cm, and that the mean squared fluctuation in the twist angle, $\langle \phi^2 \rangle$, of a subunit located near the center of a flexible macromolecule follows the relationship (30)

$$\langle \phi^2 \rangle = 2k_B T \left( \frac{t}{\pi \alpha \gamma} \right)^{1/2}. \tag{6}$$

Here $\gamma = 6.15 \times 10^{-23}$ dyn-cm s is the friction factor for rotation of a DNA subunit about its $z$ axis, $k_B$ is the Boltzmann constant, and $T = 293$°K is the temperature. Eq. 6 is valid over a restricted time regime; however, for a molecule like phage $\lambda$ DNA, which is 50,000 base pairs in length, the above "intermediate zone" formula 6 should describe the evolution of the root mean squared twist for ~5 $\mu$s of the 10-$\mu$s bleach pulse. After 5 $\mu$s we find that

$$\langle \phi^2 \rangle^{1/2} = 148°. \tag{7}$$

Hence, anisotropy loss that originates in twisting relaxation of the DNA probably is reflected in the high value for $R(0)$ measured here.

Bending deformations of the macromolecule will also lead to anisotropy loss during both the bleach and observation periods. The bending analogue of Eq. 6 has been derived, in the small deformation limit, by Barkley and Zimm (BZ) (27). We will not invoke a BZ description here; instead our 100-$\mu$s post-bleach anisotropy decay will be compared (qualitatively) to a selection of experimen-

tally observed microsecond and millisecond reorientational relaxations of long DNA molecules. We will focus on light scattering and dichroism studies rather than the transient singlet depletion work because the latter technique has been used to probe the motion of molecules that are very much shorter than phage λ DNA.

Ding et al. have looked at the decay of electrically induced dichroism in DNA samples consisting of molecules that are a factor of 5 shorter than phage λ DNA (2). Similarly, Callis and Davidson have conducted flow dichroism studies on DNA molecules with molecular weights (M.W.) in the range ($1.2 \times 10^7 <$ M.W. $< 1.25 \times 10^8$) (3). Finally, Schmitz and Schurr have examined the rotational relaxation of a long DNA (M.W. = $1.5 \times 10^7$) with the dynamic light scattering technique (8). In each of these studies, it was concluded that the polymer exhibits a spectrum of reorientational relaxations and that the long-time (millisecond) tail of the rotational recovery was adequately described by the Rouse-Zimm (RZ) coil deformation model (31, 32). In the RZ model the very large amplitude reorientations of a polymer are characterized by a set of normal modes, $m$. The spatial variation in the normal coordinates is given by a simple sinusoidal function; hence, the lowest order mode contains no nodes and corresponds to a large amplitude motion of the polymer. Higher values of $m$ are associated with progressively more and more nodes in the spatial variables and describe more local polymer deformations. The characteristic Langevin relaxation time, $\tau_m$, and mean squared amplitude, $\langle \delta_m^2 \rangle$, of mode $m$ are related to known properties of the polymer as follows (for simplicity we neglect hydrodynamic effects) (33):

$$\tau_m = \frac{2R_G^2}{\pi^2 m^2 D_0} \tag{8}$$

$$\langle \delta_m^2 \rangle = \frac{N R_G^2}{6\pi^2 m^2}. \tag{9}$$

Here $R_G$ and $D_0$ are, respectively, the radius of gyration and translational diffusion coefficient of a DNA composed of $N + 1$ bead subunits. For a molecule with a molecular weight of $10^7$ the longest wavelength RZ mode will relax characteristically in tens of milliseconds. Just such a slow reorientation has been detected in dichroism and scattering studies and attributed to the $m = 1$ RZ mode. However, the FPR anisotropy decayed characteristically in 100 μs; therefore, the very large amplitude coil deformations of phage λ DNA probably were not resolved by this technique. Moreover, any RZ modes that do contribute to our 100-μs signal should be of substantially higher order than the longest wavelength motion.

Microsecond rotational relaxation of the DNA was also prominently manifested in the dichroism and light scattering experiments. For example, Schmitz and Schurr point to a short time light scattering correlation function, of appreciable amplitude, which decays in the 20–40-μs time regime. Ding et al. decompose their dichroism decay data into a sum of three exponential terms. One of the time constants reflects the $m = 1$ RZ mode. An 8-μs relaxation that is independent of molecular weight was also detected. This decay was attributed to independent rotational motion of a piece of DNA of ~250 base pairs in length. Finally, an intermediate relaxation time, which is a monotonically increasing function of molecular weight, was also observed. For example, 34% of the signal derived from a DNA (M.W. = $6.7 \times 10^6$) was attributed to a 197-μs relaxation. This middle correlation time was assumed to reflect a complex superposition of rotational motions.

It is likely that our 100-μs post-bleach recovery of phage λ DNA is also a manifestation of a "spectrum of reorientational processes." An 8-μs independent motion of DNA segments should relax during the bleach pulse. We emphasize again that the FPR experiment probes a rather complex set of angular quantities and, therefore, it is hard to make a quantitative comparison between our data and published theoretical and experimental work. Nevertheless, these polarized FPR experiments, and a variety of other spectroscopic studies, suggest that long DNA molecules undergo large amplitude reorientations in the microsecond time regime.

## CONCLUSIONS

Fluorescence spectroscopy provides one of the most sensitive ways to monitor the dynamics of DNA. However, most fluorescence work on the reorientation of nucleic acids has been hampered by an inability to resolve microsecond and millisecond rotational relaxations. To overcome this limitation, we have conducted a study of DNA rotation with a fluorescence photobleaching technique that can, in principle, be used to probe the entire spectrum of motions exhibited by complex polymers. Our FPR work on an ethidium azide labeled λ DNA system indicates that, in solution, the dye/DNA complex undergoes fast motions that tend to blur the pattern of bleached molecules about that expected from a static system. Nevertheless, a short (10 μs) pulse of intense light creates a detectable anisotropy in the angular distribution of ethidium azide labeled λ DNA. The dye concentration then returns to angular uniformity as the DNA experiences post-bleach rotation. With the FPR technique we were able to follow the reorientational motions of phage λ DNA which relax characteristically within 120 μs.

## APPENDIX 1

### Discussion of Eq. 3

In this appendix we will sketch a formal, but realistic, model of the FPR-DNA signal. This discussion will serve also to illustrate the nature of the angular averages that characterize the polarized FPR experiment. (Recall that the FPR and fluorescence depolarization signals do not reflect exactly the same angular expectation values.)

Consider a parallel mode FPR experiment. The angle, $\alpha$, between the absorption dipole of the dye and the $y$-polarized bleach beam will in

general vary during the bleach pulse (and the lifetime of the excited state); therefore the probability that a fluorophore is unbleached at time $t'$ is written

$$P(t') = \exp\left[-B\int_0^{t'} p(t_1)\cos^2\alpha(t_1)\,dt_1\right]. \quad \text{(A1)}$$

Here $B$ is a parameter that depends on the intensity of the bleaching beam and $p(t_1)$ is a normalized pulse shape. In the parallel mode the probability of exciting a dye molecule at time $t'$, with probe light, is proportional to $\cos^2\alpha(t')$. Finally, the rate of emission (along $\hat{\mathbf{y}}$) at time $t''$ from a fluorophore that absorbed a photon at $t'$ is proportional to the quantity

$$\cos^2\alpha(t'')\frac{1}{\tau_f}\exp\left[-\frac{t''-t'}{\tau_f}\right]. \quad \text{(A2)}$$

In expression A2, $\tau_f$ is the lifetime of the chromophore.

We can now write the parallel mode FPR-DNA signal from a particular chromophore as

$$F_{DNA}(t) \propto \int_0^t \left\langle \exp\left[-B\int_0^{t'} p(t_1)\cos^2\alpha(t_1)\,dt_1\right] \cdot \frac{1}{\tau_f}\exp\left[-\frac{t-t'}{\tau_f}\right]\cos^2\alpha(t')\cos^2\alpha(t)\right\rangle dt'. \quad \text{(A3)}$$

The angle brackets ($\langle\ \rangle$) denote an ensemble average.

If it is assumed that the molecules are immobile during the excited state lifetime and the bleach pulse, and that relaxation is governed by isotropic spherical rotational diffusion, Eq. 3 in the text will follow from A3 and its perpendicular mode analogue.

## APPENDIX 2
## Derivation of Eq. 4

Throughout this mathematical discussion the polarizations of the parallel and perpendicular mode bleaching beams will define the directions of the laboratory $z$ and $y$ axes. The polarization of the probe beam must then be parallel to $z$. (Note that these choices for the direction of the bleach and probe beam polarization are not the same as the convention established in the text or Appendices 1 and 3. However, we make this change so that all angular variables can be interpreted as spherical polar coordinates.) In our experimental configuration only the $z$ component of the fluorescence is passed to the photomultiplier.

Consider an absorption dipole that wobbles in a cone of half angle $\alpha$ during the bleach pulse and the first 10-$\mu$s interval over which excitation counts are collected. The cone is centered on an axis whose polar and azimuthal angles in the laboratory frame are $\theta_0$ and $\phi_0$ (see Fig. 3). The orientation of the absorption moment (not the cone) is time dependent and will be denoted by $(\theta, \phi)$.

We analyze the effect of wobble on the initial ratio in the "weak" bleach limit. The probability that the dye molecule is bleached by $z$-polarized light is then proportional to the ensemble average of $\cos^2\theta$ over the wobble cone. Similarly the probability that the fluorophore is bleached by $y$-polarized light is proportional to $\langle\sin^2\theta\sin^2\phi\rangle$. Moreover, if it is assumed that the average orientation of the transition moment does not change significantly as the phototube reopens and the first set of observation counts is collected, the excitation of the dye molecule by the probe beam is also proportional to the average of $\cos^2\theta$ over the bleach cone. Finally only the $z$ component of the fluorescence is actually passed to the photomultiplier; therefore the detection geometry will also introduce a factor of $\langle\cos^2\theta\rangle$ into the expression for the fluorescence signal. (We assume here that the absorption and emission moments are parallel.) The problem is, then, to evaluate $\langle\cos^2\theta\rangle$ and $\langle\sin^2\theta\sin^2\phi\rangle$ and to determine what effect these quantities have on the initial ratio.

It is most convenient to compute the required expectation values in a coordinate system whose $z$ axis is along the average position of the transition moment $(\theta_0, \phi_0)$. We need, therefore, to establish the relationship between the coordinates of a point in the laboratory and wobble frames. The laboratory axes are coincident with the wobble axes after a counterclockwise rotation through an angle $3\pi/2 + \phi_0$ about the laboratory $z$ axis; this first rotation is then followed by a counterclockwise rotation of $2\pi - \theta_0$ about the new $x$ axis. Thus the coordinates of a vector relative to the molecular (primed) axes are related to the components of the vector in the laboratory (unprimed) frame by the matrix equation (34)

$$\begin{pmatrix} x \\ y \\ z \end{pmatrix} = \begin{pmatrix} \sin\phi_0 & \cos\phi_0\cos\theta_0 & \sin\theta_0\cos\phi_0 \\ -\cos\phi_0 & \cos\theta_0\sin\phi_0 & \sin\theta_0\sin\phi_0 \\ 0 & -\sin\theta_0 & \cos\theta_0 \end{pmatrix}\begin{pmatrix} x' \\ y' \\ z' \end{pmatrix}. \quad \text{(B1)}$$

We require the quantities $\langle\sin^2\theta\sin^2\phi\rangle = \langle(y/r)^2\rangle$ and $\langle\cos^2\theta\rangle = \langle(z/r)^2\rangle$. Here $r$ is just the conventional radial polar coordinate of a point. We will use the transformation Eq. B1 to rewrite these expectation values in terms of primed (wobble) coordinates. From B1 it follows that

$$z = -\sin\theta_0 y' + \cos\theta_0 z' \quad \text{(B2)}$$

and

$$y = -\cos\phi_0 x' + \cos\theta_0\sin\phi_0 y' + \sin\theta_0\sin\phi_0 z'. \quad \text{(B3)}$$

Moreover, if $(\theta', \phi')$ specifies the orientation of the transition moment in the molecular frame, we have

$$x' = r\sin\theta'\cos\phi'; \qquad y' = r\sin\theta'\sin\phi'; \qquad z = r\cos\theta'. \quad \text{(B4)}$$

After substitution of the relationships B4 into Eqs. B2 and B3, the resulting expressions for $z$ and $y$ can be used to demonstrate that

$$\begin{aligned}\langle\sin^2\theta\sin^2\phi\rangle = {} & \cos^2\phi_0\langle\sin^2\theta'\cos^2\phi'\rangle + \cos^2\theta_0\sin^2\phi_0 \\ & \cdot\langle\sin^2\theta'\sin^2\phi'\rangle + \sin^2\theta_0\sin^2\phi_0\langle\cos^2\theta'\rangle \\ & -\cos\phi_0\cos\theta_0\sin\phi_0\langle\sin^2\theta'\cos\phi'\sin\phi'\rangle \\ & -\sin\theta_0\sin\phi_0\cos\phi_0\langle\sin\theta'\cos\theta'\cos\phi'\rangle \\ & +\cos\theta_0\sin\theta_0\sin^2\phi_0\langle\cos\theta'\sin\theta'\sin\phi'\rangle \end{aligned} \quad \text{(B5)}$$

and

$$\begin{aligned}\langle\cos^2\theta\rangle = {} & \sin^2\theta_0\langle\sin^2\theta'\sin^2\phi'\rangle + \cos^2\theta_0\langle\cos^2\theta'\rangle \\ & -2\sin\theta_0\cos\theta_0\langle\sin\theta'\sin\phi'\cos\theta'\rangle. \end{aligned} \quad \text{(B6)}$$

The simplification achieved by the transformation into the molecular frame is now evident. Evaluation of expressions B5 and B6 simply requires computation of the ensemble average of functions of molecule-referenced angular variables. These averages will be the same for all transition dipoles; if the expectation values were evaluated in the laboratory frame the answers would, of course, depend on the average orientation of the wobble axis.

The expectation values are easily evaluated analytically for a uniform motion model. In this case it is clear that the amount of time spent in a small area $d\Omega'$ about $(\theta', \phi')$ is simply proportional to the area $d\Omega'$. Hence we compute the averages in Eqs. B5 and B6 as integrals over $d\Omega' = \sin\theta'\,d\theta'\,d\phi'$. The probability of finding a dipole with a given orientation is normalized to the total area of the cone. The limits of integration are simply $0 < \theta' < \alpha$ and $0 < \phi' < 2\pi$. The last three terms in expression B5 and the final integral in B6 all vanish when $\phi'$ ranges from 0 to $2\pi$. After explicit evaluation of the nonzero integrals, it is found that

$$\langle\sin^2\theta\sin^2\phi\rangle = \frac{\cos\alpha(\cos\alpha+1)}{2}\left(\sin^2\theta_0\sin^2\phi_0 - \frac{1}{3}\right) + \frac{1}{3} \quad \text{(B7)}$$

and

$$\langle \cos^2\theta \rangle = \frac{\cos\alpha(\cos\alpha + 1)}{6}(3\cos^2\theta_0 - 1) + \frac{1}{3}. \quad \text{(B8)}$$

We can now use these uniformly averaged angular quantities to compute the initial ratio as a function of wobble angle. Recall that $R(0)$ is defined as

$$R(0) = \frac{F_0 - F_\perp(0)}{F_0 - F_\parallel(0)} = \frac{1 - \dfrac{F_\perp(0)}{F_0}}{1 - \dfrac{F_\parallel(0)}{F_0}}. \quad \text{(B9)}$$

In the low bleach limit the quantity $F_\perp(0)/F_0$ is given by (see Appendix 1) the following expression:

$$\frac{F_\perp(0)}{F_0} = \frac{\int_0^{2\pi}\int_0^{\pi}(1 - B\langle \sin^2\theta\sin^2\phi\rangle)\langle\cos^2\theta\rangle^2\sin\theta_0 d\theta_0 d\phi_0}{\int_0^{2\pi}\int_0^{\pi}(\langle\cos^2\theta\rangle^2\sin\theta_0 d\theta_0 d\phi_0)}. \quad \text{(B10)}$$

The last step in the calculation involves inserting our expressions for the wobble-averaged angular quantities into the equations for $F_\perp/F_0$ and $F_\parallel/F_0$ and then computing the integrals over $\theta_0$ and $\phi_0$. Eq. B9 can then be used to find $R(0)$ as a function of $\alpha$.

## APPENDIX 3

## Derivation of Eq. 5

An exact calculation of the maximal temperature rise in a three-dimensional absorbing sample that is illuminated with light having a diverging gaussian intensity profile is complicated. Therefore in this analysis of thermal effects we make two approximations both of which will lead to an overestimate of the maximal bleach-induced temperature increase. First, the divergence of the beam is neglected. Second, we compute an approximate $\Delta T$ given by the product of the initial rate of temperature increase multiplied by the length of the bleach pulse.

The temperature distribution is governed by the inhomogeneous diffusion equation

$$-\frac{\partial T(\mathbf{r}, t)}{\partial t} + \kappa\nabla^2 T(\mathbf{r}, t) = \frac{A(\mathbf{r}, t)}{c_p\rho}. \quad \text{(C1)}$$

In Eq. C1 $A(\mathbf{r}, t)$ is the power per unit volume deposited by the laser beam at point $\mathbf{r}$ at time $t$ and $\kappa$ is the thermal diffusivity of the medium. If the heat source has a nondiverging gaussian intensity profile then $A(\mathbf{r}, t) = (4.6\epsilon CP/\pi\omega_0^2)\exp(-2r^2/\omega_0^2)$. Here $r$ is the standard radial cylindrical distance of point $\mathbf{r}$ from the position of maximal light intensity.

We compute the temperature profile by integrating the three-dimensional free space Green's function of Eq. C1 over the inhomogeneous term $A(\mathbf{r}, t)$. The Green's function of C1 is

$$G(\mathbf{r} - \mathbf{r}', t - t') = \frac{1}{[4\pi\kappa(t - t')]^{3/2}}\exp\left[\frac{-(\mathbf{r} - \mathbf{r}')^2}{4\kappa(t - t')}\right] \quad t > t'$$
$$G(\mathbf{r} - \mathbf{r}', t - t') = 0 \quad t < t'. \quad \text{(C2)}$$

Hence the solution of C1 may be written

$$T(\mathbf{0}, t) = \int_0^t dt' \int d\mathbf{r}' G(\mathbf{0} - \mathbf{r}', t - t')\frac{A(\mathbf{r}', t')}{c_p\rho}. \quad \text{(C3)}$$

For our particular choice of $A(\mathbf{r}, t)$ Eq. C3 reads

$$T(\mathbf{0}, t) = B\int_0^t dt' \int_{-\infty}^{\infty} dz' \int_0^{\infty} dr' \cdot \frac{2\pi r'}{[4\pi\kappa(t - t')]^{3/2}}\exp\left[\frac{-r'^2 - z'^2}{4\kappa(t - t')}\right]\exp\left(\frac{-2r'^2}{\omega_0^2}\right) \quad \text{(C4)}$$

where $B = 4.6\epsilon CP/\pi\omega_0^2 c_p\rho$. We make the change of variable $\beta = 1/\sqrt{t - t'}$. It follows that

$$T(\mathbf{0}, t) = \frac{4\pi B}{[4\pi\kappa]^{3/2}}\int_{t^{-1/2}}^{\infty} d\beta \int_{-\infty}^{\infty} dz' \int_0^{\infty} dr' r' \cdot \exp\left[-r'^2\left(\frac{\beta^2}{4\kappa} + \frac{2}{\omega_0^2}\right)\right]\exp\left(\frac{-z'^2\beta^2}{4\kappa}\right). \quad \text{(C5)}$$

We are interested in determining the bleach-induced temperature rise, $\Delta T$, at the position of maximal beam intensity ($r = 0$). We have the approximate relationship $\Delta T = dT/dt\ \Delta t$ where $dT/dt$ is the rate of temperature increase at $t = 0$ and $r = 0$; $\Delta t$ is the length of the bleach. The derivative of the temperature with respect to time may be determined from the chain rule. It follows that

$$\frac{dT}{dt} = \frac{1}{2}t^{-3/2}\frac{4\pi B}{[4\pi\kappa]^{3/2}}\int_{-\infty}^{\infty} dz' \int_0^{\infty} dr' r' \cdot \exp\left[-r'^2\left(\frac{1}{4\kappa t} + \frac{2}{\omega_0^2}\right)\right]\exp\left(\frac{-z'^2}{4\kappa t}\right). \quad \text{(C6)}$$

Evaluation of the integral over $r'$ yields the following expression

$$\frac{dT}{dt} = \pi B t^{-3/2}(4\pi\kappa)^{-3/2}\int_{-\infty}^{\infty} dz' \frac{\exp\left(\dfrac{-z'^2}{4\kappa t}\right)}{\dfrac{2}{\omega_0^2} + \dfrac{1}{4\kappa t}}. \quad \text{(C7)}$$

Finally, if the integral over $z'$ is computed it is found that

$$\frac{dT}{dt} = \frac{2B}{1 + \dfrac{8\kappa t}{\omega_0^2}}. \quad \text{(C8)}$$

Note that the rate of temperature increase at $r = 0$ is maximal at $t = 0$. An upperbound for the bleach-induced temperature rise is therefore

$$\Delta T = 2B\Delta t = \frac{9.2\epsilon CP}{\pi\omega_0^2 c_p\rho}\Delta t. \quad \text{(C9)}$$

More precisely we have the following explicit expression for $T(0, t)$

$$T(0, t) = \frac{2.3\epsilon CP}{2\pi\kappa c_p\rho}\ln\left(1 + \frac{8\kappa t}{\omega_0^2}\right). \quad \text{(C10)}$$

Eq. C9 is merely the short time limit of Eq. C10.

We are pleased to acknowledge Aaron B. Kantor, Patricia Maxson, and Meredith Morgan for their help with the spectrofluorimetry. We also thank Michael J. Saxton for many helpful references and discussions, and James R. Abney and the referees for a critical reading of the manuscript.

This work was supported by National Institutes of Health grants GM30781 (J. E. Hearst) and NS14565 (D. Axelrod), and by the Office of Energy Research, Office of Health and Environmental Research of the U.S. Dept. of Energy under contract number DE AC03-76SF00098. This

research was also conducted in part by an appointment (B. A. Scalettar) to the Alexander Hollaender Distinguished Postdoctoral Fellowship Program supported by the U.S. Department of Energy, Office of Health and Environmental Research, and administered by Oak Ridge Associated Universities. P. Selvin was supported by a National Science Foundation fellowship.

*Received for publication 29 December 1986 and in final form 15 October 1987.*

## REFERENCES

1. Cantor, C. R., and P. R. Schimmel. 1980. Biophysical Chemistry III. W.H. Freeman and Co., San Francisco. 1031–1033.
2. Ding, D., R. Rill, and K. E. Van Holde. 1972. The dichroism of DNA in electric fields. *Biopolymers.* 11:2109–2124.
3. Callis, P. R., and N. Davidson. 1969. Hydrodynamic relaxation times of DNA from decay of flow dichroism measurements. *Biopolymers.* 8:379–390.
4. Thompson, D. S., and S. J. Gill. 1967. Polymer relaxation times from birefringence relaxation measurements. *J. Chem. Phys.* 47:5008–5017.
5. Diekmann, S., W. Hillen, B. Morgeneyer, R. D. Wells, and D. Porschke. 1982. Orientation relaxation of DNA restriction fragments and the internal mobility of the double helix. *Biophys. Chem.* 15:263–270.
6. Elias, J. G., and D. Eden. 1981. Transient electric birefringence study of the persistence length and electrical polarizability of restriction fragments of DNA. *Macromolecules.* 14:410–419.
7. Hagerman, P. J. 1981. Investigation of the flexibility of DNA using transient electric birefringence. *Biopolymers.* 20:1503–1535.
8. Schmitz, K. S., and J. M. Schurr. 1973. Rotational relaxation of macromolecules determined by dynamic light scattering. II. Temperature dependence for DNA. *Biopolymers.* 12:1543–1564.
9. Lewis, R. J., J. H. Huang, and R. Pecora. 1985. Rotational and translational motion of supercoiled plasmids in solution. *Macromolecules.* 18:944–948.
10. Lewis, R. J., R. Pecora, and D. Eden. 1986. Transient electric birefringence measurements of the rotational and internal bending modes in monodisperse DNA fragments. *Macromolecules.* 19:134–139.
11. Wahl, Ph., J. Paoletti, and J. B. Le Pecq. 1970. Decay of fluorescence emission anisotropy of the ethidium bromide DNA complex. Evidence for internal motion in DNA. *Proc. Natl. Acad. Sci. USA.* 65:417–421.
12. Genest, D., and P. Wahl. 1978. Fluorescence anisotropy decay due to rotational Brownian motion of ethidium intercalated in double strand DNA. *Biochem. Biophys. Acta.* 521:502–509.
13. Thomas, J. C., S. A. Allison, C. J. Appellof, and J. M. Schurr. 1980. Torsion dynamics and depolarization of fluorescence of linear macromolecules. II. Fluorescence polarization anisotropy measurements on a clean viral $\phi 29$ DNA. *Biophys. Chem.* 12:177–188.
14. Millar, D. P., R. J. Robbins, and A. H. Zewail. 1980. Direct observation of the torsional dynamics of DNA and RNA by picosecond spectroscopy. *Proc. Natl. Acad. Sci. USA.* 77:5593–5597.
15. Hogan, M. E., and O. Jardetzky. 1979. Internal motions in DNA. *Proc. Natl. Acad. Sci. USA.* 76:6341–6345.
16. Bolton, P. H., and T. L. James. 1980. Fast and slow conformational fluctuations of RNA and DNA. Subnanosecond internal motion correlation times determined by $^{31}P$ NMR. *J. Am. Chem. Soc.* 102:25–31.
17. Early, T. A., and D. R. Kearns. 1979. $^{1}H$ Nuclear magnetic resonance investigation of flexibility in DNA. *Proc. Natl. Acad. Sci. USA.* 76:4165–4169.
18. Magde, D., M. Zappala, W. H. Knox, and T. M. Nordlund. 1983. Picosecond fluorescence anisotropy decay in the ethidium/DNA complex. *J. Phys. Chem.* 87:3286–3288.
19. Hogan, M., J. Wang, R. H. Austin, C. L. Monitto, and S. Hershkowitz. 1982. Molecular motion of DNA as measured by triplet anisotropy decay. *Proc. Natl. Acad. Sci. USA.* 79:3518–3522.
20. Smith, L. M., R. M. Weis, and H. M. McConnell. 1981. Measurement of rotational motion in membranes using fluorescence recovery after photobleaching. *Biophys. J.* 36:73–91.
21. Graves, D. E., L. W. Yielding, C. L. Watkins, and K. L. Yielding. 1977. Synthesis, separation and characterization of the monoazide and diazide analogs of ethidium bromide. *Biochem. Biophys. Acta.* 479:98–104.
22. Magde, D., E. L. Elson, and W. W. Webb. 1974. Fluorescence correlation spectrospecy. II. An experimental realization. *Biopolymers.* 13:29–61.
23. Wegener, W. A., and R. Rigler. 1984. Separation of translational and rotational contributions in solution studies using fluorescence photobleaching recovery. *Biophys. J.* 46:787–793.
24. Dale, R. E. 1987. Depolarized fluorescence photobleaching recovery. *Eur. Biophys. J.* 14:179–193.
25. Axelrod, D. 1979. Carbocyanine dye orientation in red cell membrane studied by microscopic fluorescence polarization. *Biophys. J.* 26:557–574.
26. Schurr, J. M. 1984. Rotational diffusion of deformable macromolecules with mean local cylindrical symmetry. *Chem. Phys.* 84:71–96.
27. Barkley, M. D., and B. H. Zimm. 1979. Theory of twisting and bending of chain macromolecules; analysis of the fluorescence depolarization of DNA. *J. Chem. Phys.* 70:2991–3007.
28. Allison, S. A., and J. M. Schurr. 1979. Torsion dynamics and depolarization of fluorescence of linear macromolecules I. Theory and application to DNA. *Chem. Phys.* 41:35–59.
29. Yoshizaki, T., M. Fujii, and H. Yamakawa. 1985. Dynamics of helical worm-like chains. VI. Fluorescence depolarization. *J. Chem. Phys.* 82:1003–1013.
30. Allison, S. A., J. H. Shibata, J. Wilcoxon, and J. M. Schurr. 1982. NMR relaxation in DNA. I. The contribution of torsional deformation modes of the elastic filament. *Biopolymers.* 21:729–762.
31. Rouse, P. E. 1953. A theory of the linear viscoelastic properties of dilute solutions of coiling polymers. *J. Chem. Phys.* 21:1272–1280.
32. Zimm, B. H. 1956. Dynamics of polymer molecules in dilute solution: viscoelasticity, flow birefringence and dielectric loss. *J. Chem. Phys.* 24:269–278.
33. Berne, B. J., and R. Pecora. 1976. Dynamic Light Scattering. John Wiley & Sons, Inc., New York. 182–188.
34. Goldstein, H. 1950. Classical Mechanics. Addison-Wesley Press, Inc., Cambridge, MA. 109.